

Calculating Stress & Strain from Experimental ODS Data

Brian Schwarz, Shawn Richardson, Mark Richardson

Vibrant Technology, Inc.

Scotts Valley, CA

[Click here](#) for the presentation

ABSTRACT

In this paper it is shown how a Finite Element Analysis (FEA) model can be used together with experimental Operating Deflection Shape (ODS) data to calculate stresses & strains in a machine or mechanical structure. This allows for the on-line monitoring of structural stress & strain, which can be compared with prescribed warning levels to insure that dangerous levels are not exceeded. Examples are included to illustrate how ODS data measured with multiple accelerometers can be used to calculate stress & strain. Also, when this data is displayed together an ODS in animation on a 3D model of the machine or structure, high levels of stress or strain, or “*hot spots*”, are quickly observed.

KEY WORDS

Operating Deflection Shape (ODS)
Stress & Strain
Finite Element Analysis (FEA) Model
FEA Mode Shapes
Modal Assurance Criterion (MAC)

INTRODUCTION

In a rotating machine, the dominant forces are applied at multiples of the machine running speed, called orders. An *order-tracked ODS* is assembled from the peaks at one of the order frequencies in a set of response frequency spectra of a machine. When displaying in animation on a 3D model, an order-tracked ODS is a convenient way to visualize vibration levels, and therefore monitor the health of the machine.

In a companion paper [2], it is shown how *modes participate* in an order-tracked ODS of a rotating machine, and how they participate differently at different operating speeds. It is also shown how the *modal participation* can be used to *expand* an order-tracked ODS so that it is suitable for display on a model of the machine.

It is well known that most rotating machines will exhibit different vibration levels under different loads and speeds. ODS's are conveniently acquired by attaching multiple accelerometers to the machine surfaces, and acquiring vibration data from the machine while it is running. In addition to visualizing the deflection of the machine in real time, an ODS can be used to calculate stress & strain by *deflecting an FEA model* of the machine.

VARIABLE SPEED ROTATING MACHINE

Figure 1 shows a variable speed rotating machine, instrumented with eight tri-axial accelerometers. An accelerometer is attached to the top of each bearing block, and six accelerometers are attached to the base plate; three on the front edge and three on the back edge. This test setup was used to measure order-tracked ODS's under different machine speeds.

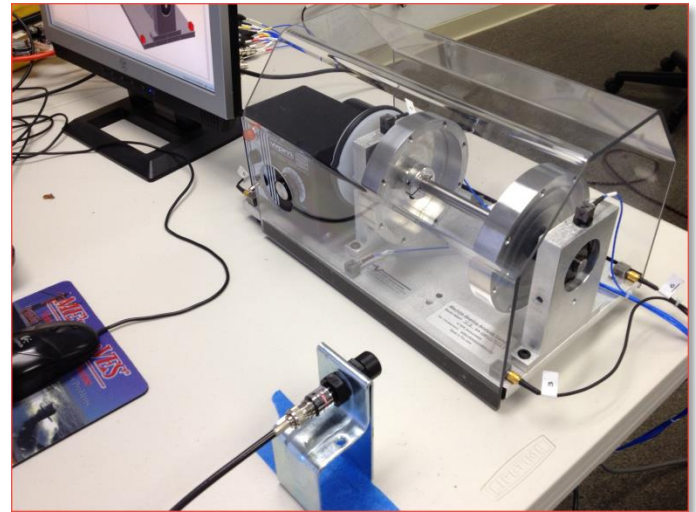


Figure 1. Variable Speed Rotating Machine

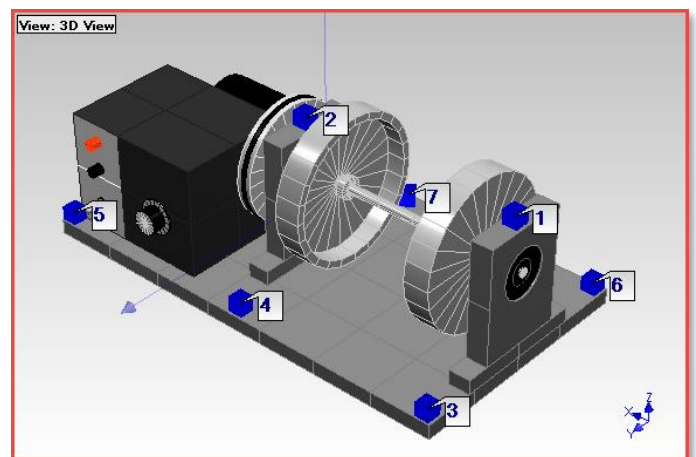


Figure 2 Rotating Machine Model.

A laser tachometer with its beam pointed at the outer wheel of the machine was used to measure the machine speed, as shown

in Figure 1. The outer wheel had reflective tape on it, so the laser measured the once-per-revolution speed of the machine.

Figure 2 contains a model of the machine that was used to display ODS's in animation. Each of the numbered test points is displayed as a cube icon.

MODE SHAPES OF THE MACHINE

The order-tracked ODS's of the machine in Figure 1 contain participation of both "rigid body" and "flexible" mode shapes of the base plate and bearing blocks. Since the machine is resting on four rubber mounts (one under each corner), its rigid body modes will participate significantly in its ODS. The machine has *six rigid body* mode shapes that describe its *free-free motion* in space, but they also participate in its ODS since it is resting on *four soft springs*.

The rigid body and flexible body mode shapes of the machine were obtained from an FEA model of the base plate and one of the bearing blocks. The first 20 mode shapes of the base plate together with 20 modes for each of the bearing blocks were used together with the SDM method [7] to solve for the modes of the combined substructures. Paper [2] contains more details of this procedure.

Select Shape	Frequency (or Time)	Units	Damping (%)	DOFs	Measurement Type	Units	Shape 1 Magnitude	Phase
1	0	Hz	0	3X	UMM Mode Shape	in/bf-sec	1.2648	0
2	0	Hz	0	3Y	UMM Mode Shape	in/bf-sec	0.83429	0
3	0	Hz	0	3Z	UMM Mode Shape	in/bf-sec	11.456	0
4	0	Hz	0	4X	UMM Mode Shape	in/bf-sec	1.2648	0
5	0	Hz	0	4Y	UMM Mode Shape	in/bf-sec	0.034838	0
6	0	Hz	0	4Z	UMM Mode Shape	in/bf-sec	2.1085	180
7	439.76	Hz	0	5X	UMM Mode Shape	in/bf-sec	1.2648	0
8	500.96	Hz	0	5Y	UMM Mode Shape	in/bf-sec	0.76462	180
9	1103.2	Hz	0	5Z	UMM Mode Shape	in/bf-sec	15.673	180
10	1198.4	Hz	0	6X	UMM Mode Shape	in/bf-sec	0.41308	0
11	1532.4	Hz	0	6Y	UMM Mode Shape	in/bf-sec	0.83429	0
12	1826.2	Hz	0	6Z	UMM Mode Shape	in/bf-sec	14.96	0
13	1909.5	Hz	0	7X	UMM Mode Shape	in/bf-sec	0.41308	0
14	2322.1	Hz	0	7Y	UMM Mode Shape	in/bf-sec	0.034838	0
15	2575.5	Hz	0	7Z	UMM Mode Shape	in/bf-sec	1.3953	0
16	2988.2	Hz	0	8X	UMM Mode Shape	in/bf-sec	0.41308	0
17	3434.3	Hz	0	8Y	UMM Mode Shape	in/bf-sec	0.76462	180
18	3914.9	Hz	0					

Figure 3. FEA Mode Shapes of the Base Plate & Bearing Blocks.

Some of the mode shapes of the base plate and bearing blocks (60 in all) are listed in Figure 3. Notice that the first six modes are rigid body modes, with frequencies of "0".

ODS EXPANSION

ODS data was acquired from the rotating machine in Figure 1 at two different machine speeds. The mode shapes of the base plate and bearing blocks were then used to *expand* the experimental ODS's acquired from the eight accelerometers to ODS's for all DOFs on the base plate and bearing blocks.

The modal participation of the first 10 FEA modes in the 985 RPM ODS is shown in Figure 4. The modal participation factors show that the *first three modes* are the *dominant contributors* to the 985 RPM ODS. All three of these *rigid body* modes are being excited at this speed, and the machine is simply "bouncing" vertically and sideways on its rubber mounts.

The modal participation of the first 10 FEA modes in the 2280 RPM ODS is shown in Figure 5. The participation factors of modes 2, 5, and 6 indicate that they *dominate* the 2280 RPM ODS. At this higher speed, the machine is "rocking and twisting" on its rubber mounts, with more motion at the outer bearing location.

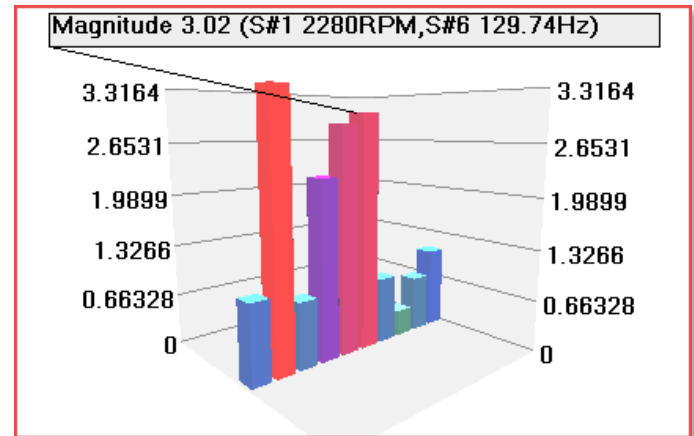


Figure 5. Magnitudes of Modal Participation at 2280 RPM.

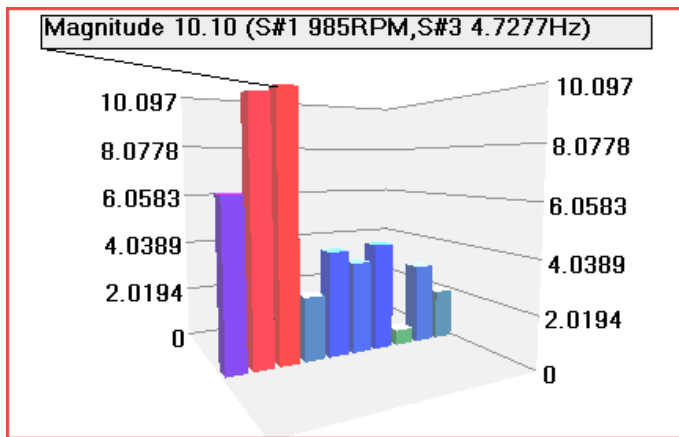


Figure 4. Magnitudes of Modal Participation at 985 RPM.

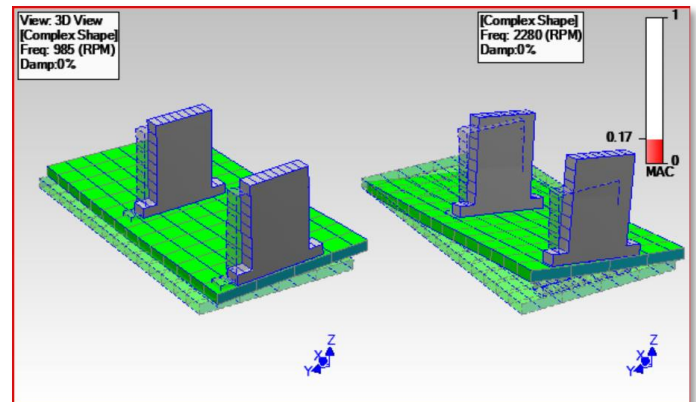


Figure 6. Expanded ODS's of Base Plate & Bearing Blocks.

Figure 6 is a comparison display of the two expanded ODS's on a model of the base plate and bearing blocks. Animation of these shapes more clearly shows that they are different, and their **low MAC value (0.17)** also indicates that they are different. The 2280 RPM ODS has much more motion at the outboard bearing block. This is due to the greater cyclic force created at the higher speed by the unbalance weight that was added to the outboard wheel.

STRAIN FROM SHAPE DATA

Strain is the forced change in the dimensions of a structure, measured as a change in **dimension per unit length**. Its units are typically **displacement per unit displacement**. Strain in an FEA element is a function of the deflections of its vertices. These deflections can be obtained from the components of an expanded ODS, or from mode shapes.

When the dynamics of a machine can be adequately represented by mode shapes, an ODS can be represented as a **weighted summation** of mode shapes. This is the well-known **superposition** property of modes.

The equation for calculating the **normal & shear strain** at an FEA element vertex is:

$$\begin{Bmatrix} \epsilon_x \\ \epsilon_y \\ \epsilon_z \\ \gamma_{xy} \\ \gamma_{yz} \\ \gamma_{xz} \end{Bmatrix} = [B] \begin{Bmatrix} u_1 \\ v_1 \\ w_1 \\ \vdots \\ u_n \\ v_n \\ w_n \end{Bmatrix} \tag{1}$$

where:

[B] = displacement strain matrix for an FEA element vertex

$$[B] = \begin{bmatrix} \frac{\partial}{\partial x} & 0 & 0 & \dots & \frac{\partial}{\partial x} & 0 & 0 \\ 0 & \frac{\partial}{\partial y} & 0 & \dots & 0 & \frac{\partial}{\partial y} & 0 \\ 0 & 0 & \frac{\partial}{\partial z} & \dots & 0 & 0 & \frac{\partial}{\partial z} \\ \frac{\partial}{\partial y} & \frac{\partial}{\partial x} & 0 & \dots & \frac{\partial}{\partial y} & \frac{\partial}{\partial x} & 0 \\ 0 & \frac{\partial}{\partial z} & \frac{\partial}{\partial y} & \dots & 0 & \frac{\partial}{\partial z} & \frac{\partial}{\partial y} \\ \frac{\partial}{\partial z} & 0 & \frac{\partial}{\partial x} & \dots & \frac{\partial}{\partial z} & 0 & \frac{\partial}{\partial x} \end{bmatrix} \tag{6 by 3n}$$

$$\begin{Bmatrix} u_1 \\ v_1 \\ w_1 \\ \vdots \\ u_n \\ v_n \\ w_n \end{Bmatrix} = \text{ODS (or mode shape) components at all vertices}$$

n = number of element vertices

$$\begin{Bmatrix} \epsilon_x \\ \epsilon_y \\ \epsilon_z \\ \gamma_{xy} \\ \gamma_{yz} \\ \gamma_{xz} \end{Bmatrix} = \text{normal \& shear strain at an FEA element vertex}$$

STRESS FROM STRAIN

Stress is the amount of **force acting within a cross sectional area** of a structure. Its units are typically **force per unit area**. Stresses are calculated from strains with the following equation:

$$\begin{Bmatrix} \sigma_x \\ \sigma_y \\ \sigma_z \\ \tau_{xy} \\ \tau_{yz} \\ \tau_{xz} \end{Bmatrix} = [C] \begin{Bmatrix} \epsilon_x \\ \epsilon_y \\ \epsilon_z \\ \gamma_{xy} \\ \gamma_{yz} \\ \gamma_{xz} \end{Bmatrix} \tag{2}$$

where:

$$\begin{Bmatrix} \sigma_x \\ \sigma_y \\ \sigma_z \\ \tau_{xy} \\ \tau_{yz} \\ \tau_{xz} \end{Bmatrix} = \text{normal \& shear stress at an FEA element vertex}$$

[C]= stress strain matrix (6 by 6)

$$[C] = \frac{E}{(1+\nu)(1-2\nu)} \begin{bmatrix} (1-\nu) & \nu & \nu & 0 & 0 & 0 \\ \nu & (1-\nu) & \nu & 0 & 0 & 0 \\ \nu & \nu & (1-\nu) & 0 & 0 & 0 \\ 0 & 0 & 0 & \frac{(1-2\nu)}{2} & 0 & 0 \\ 0 & 0 & 0 & 0 & \frac{(1-2\nu)}{2} & 0 \\ 0 & 0 & 0 & 0 & 0 & \frac{(1-2\nu)}{2} \end{bmatrix}$$

E= Young's modulus of elasticity

ν = Poisson's ratio

STRAIN FROM MODE SHAPES

The participation factors shown in Figures 4 & 5 indicate that the **flexible body** modes 7, 9, and 10 also contributed to both the 985 and 2280 RPM ODS's. Figure 7 is a display of the deflection of each of these mode shapes, together with the **normal strain in the x-direction** of the base plate and bearing blocks.

Notice that where local bending occurs in each mode shape, positive strain (**tension**) on one side of the base plate equals the same amount of negative strain (**compression**) on the other side. Also, the cross section of the plate transitions from positive to negative strain values.

STRESS FROM MODE SHAPES

Figure 8 is a display of the deflection of modes 7, 9, and 10 together with the **normal stress in the x-direction** of the base plate and bearing blocks.

Notice again that where local bending occurs, positive stress (*tensile*) on one side of the base plate equals the same amount of negative stress (*compressive*) on the other side of the plate. Also, the cross section of the plate transitions from positive to negative stress values.

STRAIN FROM THE 985 & 2280 RPM ODS's

Figure 9 is a display of the **normal strain in the x-direction** calculated for both the 985 RPM and 2280 RPM ODS's. Notice that the strain distributions of the two ODS's are different, primarily because the ODS's themselves are different, as shown in Figure 6. Also, the peak strain levels are higher for the 2280 RPM ODS, which is expected. Unlike the mode shape strain values, these values are realistic because they are based on the experimental ODS values in **inches** of displacement.

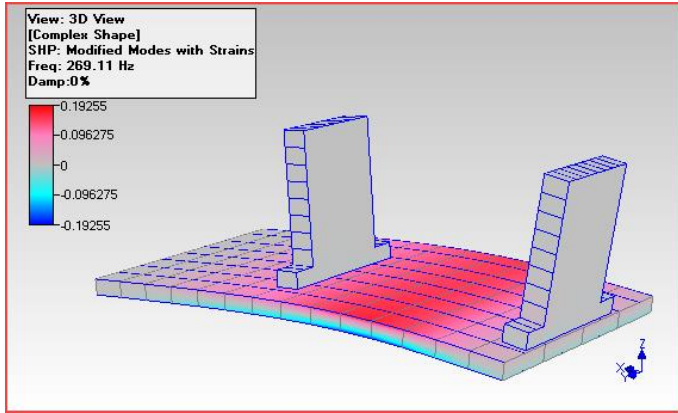


Figure 7A. Normal Strain, X-Direction, Mode #7.

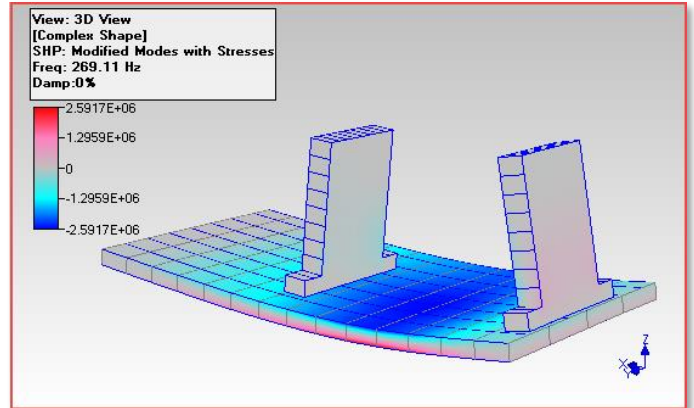


Figure 8A. Normal Stress, X-Direction, Mode #7.

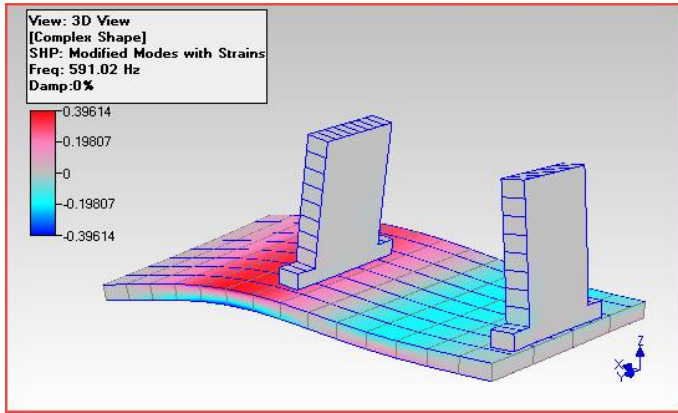


Figure 7B. Normal Strain, X-Direction, Mode #9.

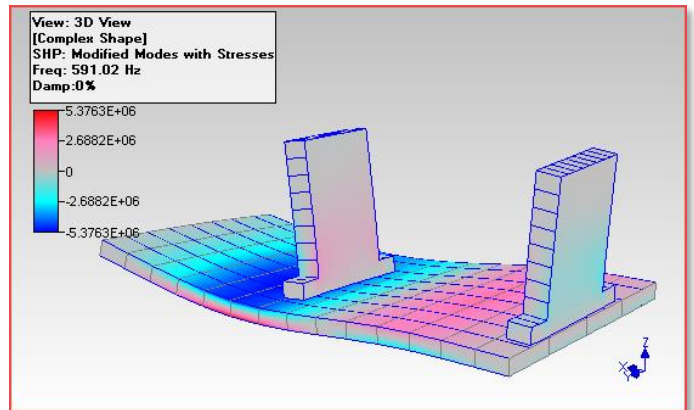


Figure 8B. Normal Stress, X-Direction, Mode #9.

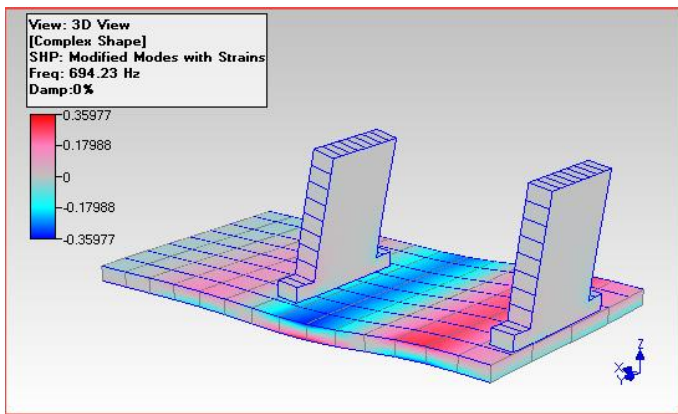


Figure 7C. Normal Strain, X-Direction, Mode #10.

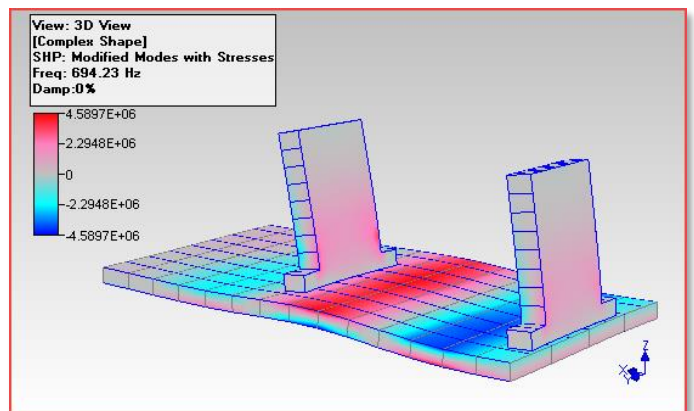


Figure 8C. Normal Stress, X-Direction, Mode #10.

STRESS FROM THE 985 & 2280 RPM ODS's

Figure 10 is a display of the **normal stress in the x-direction** calculated for both the 985 RPM and 2280 RPM ODS's. Again, the stress distribution is noticeably different between the two ODS's. The peak stress levels are also higher for the 2280 RPM ODS, as expected.

These stress values are dimensionally correct (in **psi** units) because they are based on the strain values in Figure 9, which are also dimensionally correct

neering units associated with them, they cannot be used to calculate valid stress & strain from an FEA model.

Only ODS data in displacement units will give valid stress & strain values when used to deflect an FEA model.

A key advantage of this technique is that the same FEA model can be used both for calculating the mode shapes required to expand the experimental ODS data and also for calculating stresses & strains.

When implemented as part of a troubleshooting or long term monitoring system, this technique can provide valid stress & strain data in **"real time"** under different machine operating conditions. The animated display on an ODS together with stress & strain is very useful for quickly identifying regions of high stress & strain caused by vibration.

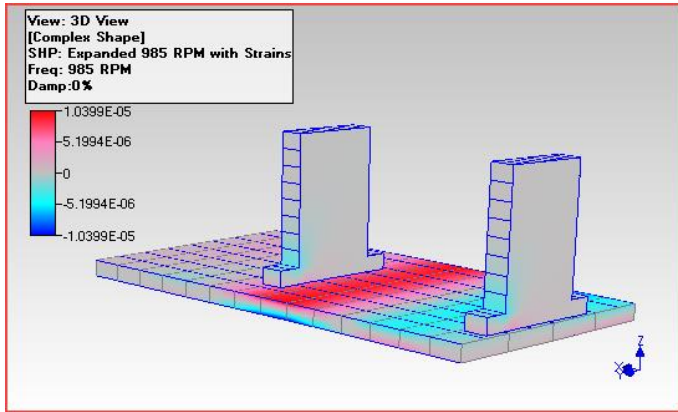


Figure 9A. Normal Strain, X-Direction, 985 RPM ODS.

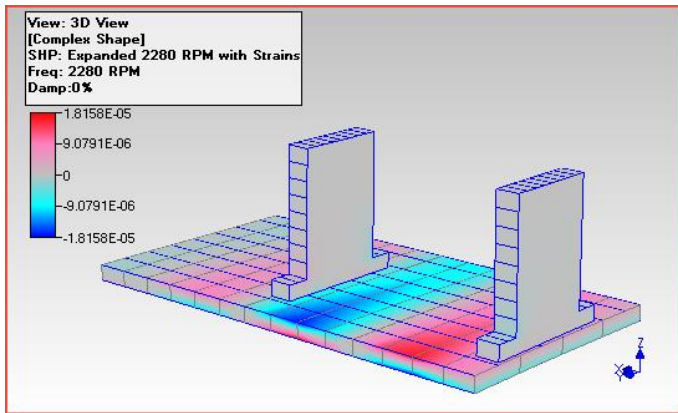


Figure 9B. Normal Strain, X-Direction, 2280 RPM ODS.

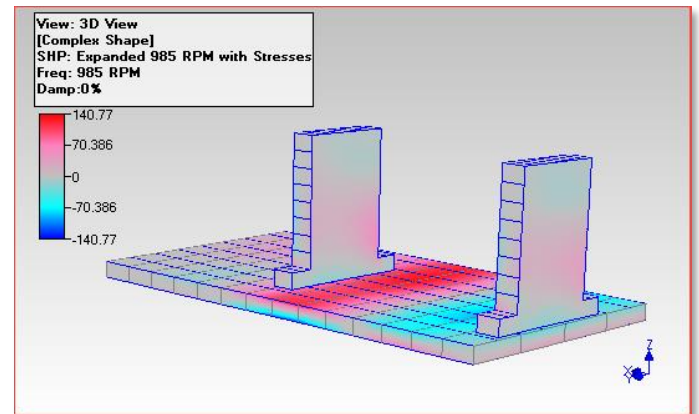


Figure 10A. Normal Stress, X-Direction, 985 RPM ODS.

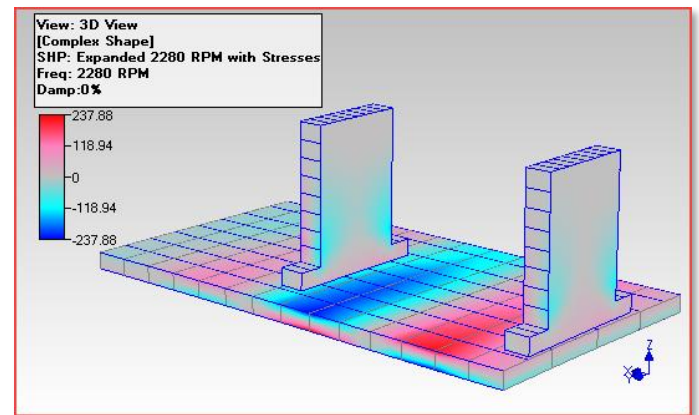


Figure 10B. Normal Stress, X-Direction, 2280 RPM ODS.

CONCLUSIONS

In this paper, it was shown how an FEA model of a machine or structure can be used to calculate stress & strain from experimental ODS data. Experimental ODS's can be acquired while a machine is running, and FEA mode shapes can be used to expand the ODS data to include all of the DOFs of the FEA mode shapes. The details of shape expansion were given in [1] & [2]. Then the FEA model was used to calculate stress & strain values by deflecting it with the expanded ODS data. Finally, it was shown that both the deflection and the stress & strain of the FEA model can be displayed together on the model.

We also showed stress & strain values together with some of the flexible modes of the base plate and bearing blocks, simply to illustrate how the FEA model yielded stress & strain when deflected. However, since mode shapes do not have any engi-

REFERENCES

1. B. Schwarz, M. Richardson, "Linear Superposition and Modal Participation" IMAC XXXII, February 3-6, 2014.
2. B. Schwarz, Shawn Richardson, Mark Richardson, "Using Mode Shapes for Real Time ODS Animation" IMAC XXXIII February 3-5, 2015.
3. S.C. Richardson, M.H. Richardson "Using Photo Modeling to Obtain the Modes of a Structure" Proceedings of the International Modal Analysis Conference, 2008.
4. M. Richardson, "Is It a Mode Shape or an Operating Deflection Shape?" Sound and Vibration magazine, March, 1997.
5. M. Richardson "Modal Analysis Versus Finite Element Analysis" Sound and Vibration Magazine, September 2005.
6. Brian J. Schwarz & Mark H. Richardson "Structural Modifications Using Higher Order Elements" 15th IMAC Conference, February, 1997.